Photon energy dependence of final state screening in a dilute electron gas system: A synchrotron radiation photoemission study of β-PbO$_2$

D.J. Payne [a], J.P. Hu [a], R.G. Egdell [a,*], V.R. Dhanak [b], G. Miller [b]

[a] *Department of Chemistry, Inorganic Chemistry Laboratory, South Parks Road, Oxford OX1 3QR, UK*
[b] *Daresbury Laboratory, Warrington, Cheshire WA4 4AD, UK*

Abstract

Photoemission spectra of thick films of β-PbO$_2$ have been measured over a range of exciting photon energies between 40 eV and 150 eV. There is evidence for occupation of conduction band states above the top of the main valence band to give a degenerate electron gas and the spectra terminate in a sharp metallic Fermi edge. Structure associated with screening of shallow 5d core holes by the mobile conduction electrons observed in Al Kα excited X-ray photoemission spectra is suppressed in the lower energy spectra and the Pb 5d core level appears as a simple spin-orbit doublet.
© 2007 Elsevier B.V. All rights reserved.

Almost all group 4 or group 14 metal dioxides are insulators with a wide gap separating a filled valence band of states with dominant O 2p atomic character from an empty conduction band of cation states. Examples include TiO$_2$, ZrO$_2$, HfO$_2$, CeO$_2$, ThO$_2$, SiO$_2$, GeO$_2$ and SnO$_2$, all of which have gaps in excess of 3 eV [1,2]. By contrast β-PbO$_2$ is a metallic conductor [3,4]. On the basis of calculations carried out within the local density approximation it has been argued that β-PbO$_2$ is intrinsically metallic due to overlap of a conduction band of Pb 6s states with the top of the valence band [5]. However, the carrier concentration is known to vary with preparation conditions, which implies partial filling of a conduction band by donor defects [6]. More recent density functional calculations using the generalised gradient approximation (GGA) suggest that stoichiometric β-PbO$_2$ is a semi-metal with a conduction band that touches but does not overlap the valence band [7,8]. However, it must be further recognised that density functional methods invariably underestimate bandgaps.

Experimentally it may be inferred (albeit indirectly) from X-ray photoemission measurements that there is a small bandgap and that the Fermi level sits between 0.4 eV and 0.7 eV above the bottom of the conduction band at a position dependent on sample pre-treatment [8]. It is necessary to invoke the presence of donor defects such as oxygen vacancies or proton interstitials in order to account for carrier concentrations of order 10^{21} cm^{-3} that lead to the occupation of the conduction band [7,8].

The mobile conduction electrons in β-PbO$_2$ have a strong influence on metal core level photoemission spectra excited with Al Kα radiation ($hv = 1486.6$ eV) [7,8]. In particular each component of the Pb 4f spin-orbit doublet in these spectra itself consists of two overlapping components. This structure can be understood in terms of the model proposed by Kotani for core ionisation in a narrow band metallic system, as shown schematically in Fig. 1 [9]. The Coulomb potential associated with the core hole pulls a localised state below the conduction band on the ionised atom. Two different final states are then possible depending on whether the localised trap state is filled by an electron from the conduction band to give a screened final state

* Corresponding author. Fax: +44 0 1865272690.
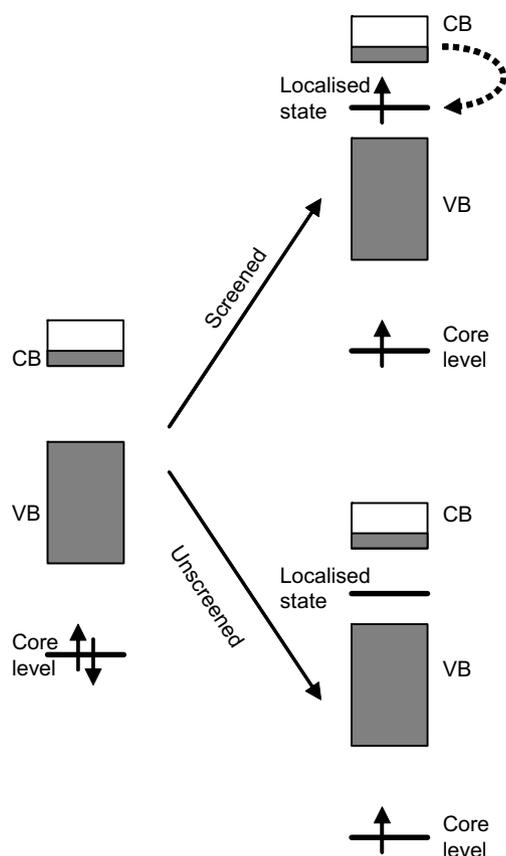 *E-mail address:* russell.egdell@chem.ox.ac.uk (R.G. Egdell).

Fig. 1. Schematic representation of final state screening of a core hole in a narrow band metallic material as described by the Kotani model.

or remains empty to give an unscreened final state. The core level structure thus comprises a low binding energy component associated with the screened final state and a lifetime broadened high binding energy component with a predominantly Lorentzian lineshape associated with the unscreened final state. The energy separation of around 1 eV between the 'screened' and 'unscreened' final states found for β-PbO$_2$ is very close to the conduction electron plasmon energy as observed in electron energy loss spectroscopy [7,8]. In this and related systems including Sb-doped SnO$_2$, Sn-doped In$_2$O$_3$ and Tl$_2$O$_3$ the 'unscreened' final state component can alternatively be described as an unusually strong plasmon satellite [10–14]: it has for many years remained a major challenge for theory to reconcile these two different viewpoints [15].

On the basis of very recent hard ($hv = 6000$ eV) X-ray photoemission experiments on correlated metallic system including V$_2$O$_3$ [16], La$_{1-x}$Sr$_x$MnO$_3$ [17], La$_{0.85}$Ba$_{0.15}$-MnO$_3$ [18] and Nd$_{2-x}$Ce$_x$CuO$_4$ [19] it appears that coherent metallic screening is strongly suppressed in the near surface region. The physics of this effect is far from clear at present, although it is now reasonably well established by empirical observation. In the present context, suppression of metallic screening near surfaces would lead to diminution of the intensity of the low binding energy core level structure under excitation with lower energy VUV synchro-

tron radiation as compared with soft X-ray excited spectra due to the greater surface sensitivity at low photon energy: the electron inelastic mean free path diminishes from about 20 Å at 1500 eV kinetic energy to values as low as about 5 Å for kinetic energies around 50 eV. On the other hand, if the outgoing photoelectron escapes from the vicinity of the core hole slow on a timescale compared with that of the screening response of the conduction electrons, the system can evolve adiabatically to reach the screened ground state of the ionised system and the low binding energy structure will predominate. In the alternative language of the plasmon model it is known that for simple metals with a high density of conduction electrons such as Al plasmon satellites are suppressed in photoemission spectra excited for outgoing electron kinetic energies below 100 eV due to interference between the intrinsic and extrinsic plasmon loss channels [20,21]. Thus, it is possible to envisage alternative scenarios which may lead to suppression of either low or high binding energy structure in core lines. Metallic PbO$_2$ provides an ideal model system in which to explore the photon energy dependence of core level screening in a dilute but uncorrelated electron gas system. In the present communication we investigate the shallow core Pb 5d lineshape in β-PbO$_2$ as a function of photon energy in the range between 50 eV and 150 eV and make comparison with the lineshape in AlKα photoemission spectra. It emerges that the distinct peaks associated with screened and unscreened states seen in AlKα XPS are not observed at low photon energy and core level structure is dominated by structure due to unscreened final states.

Films of β-PbO$_2$ with the tetragonal rutile structure [22,23] were deposited electrochemically on polished Pt substrates as described previously [7,8]. Initial surface characterisation and development of cleaning procedures were carried out in a Scienta ESCA 300 spectrometer [7,8]. This incorporates a monochromatic X-ray source. The effective instrument resolution was 350 meV.

β-PbO$_2$ has limited thermal stability and it was not possible to use standard procedures including argon ion bombardment and high temperature annealing in UHV to prepare 'clean' surfaces. However, very low levels of adventitious carbon contamination were found even without *in situ* pre-treatments, with optimal C 1s to O 1s intensity ratios as low as 1/500. Further reduction of the C 1s intensity by annealing at temperatures up to 230 °C in UHV was also possible without decomposition of the rutile phase, although such anneals did lead to an increased conduction electron concentration (see below).

Vacuum UV photoemission spectra were measured on beamline 4.1 of the synchrotron radiation source at Daresbury Laboratory UK [24]. The nominal monochromator resolution was 40 meV below $hv = 50$ eV, increasing to 120 meV at $hv = 150$ eV. The spectrometer was housed in a single chamber UHV system with a base pressure of 2×10^{-10} mbar. The chamber was equipped with a Scienta SES200 hemispherical electron energy analyser with a mean radius of 200 mm and angular acceptance of ∼10°.

The pass energy was fixed at 40 eV, giving a nominal analyser resolution of 80 meV. The chamber also included a twin anode non-monochromatised X-ray source. This enabled measurement of $MgK\alpha$ spectra with energy resolution of about 1000 meV. The $MgK\alpha$ excited Pb 4f core lines observed on the beamline showed the same structure due to final state screening as was observed in the Scienta XPS system, although the resolution was of course much poorer under non-monochromatised X-ray excitation.

Synchrotron excited valence and shallow core level spectra of a β-PbO_2 film that had been annealed progressively for 1 h at 210 °C, 220 °C and finally 230 °C are shown in Fig. 2. The $AlK\alpha$ 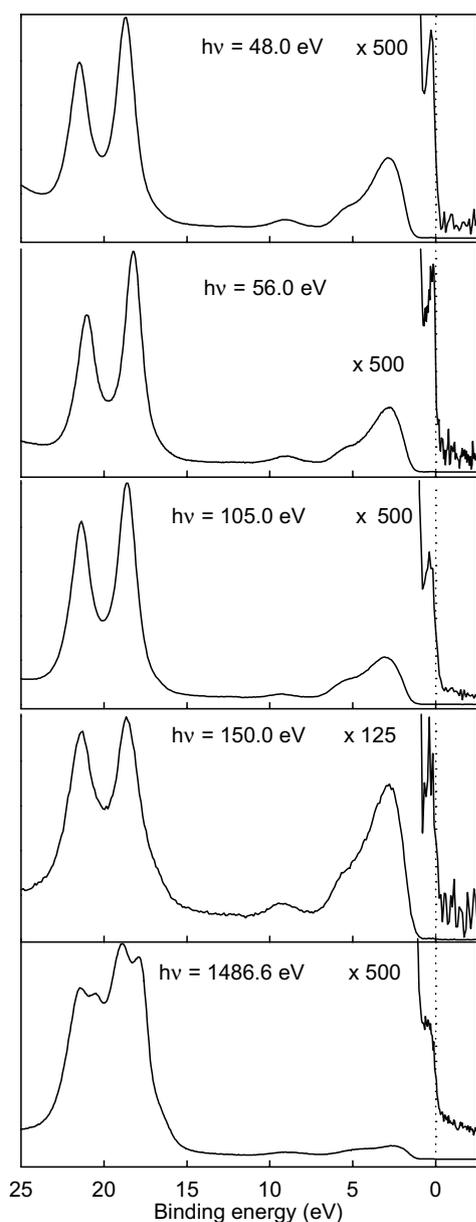spectrum of a similarly annealed sample is also shown. The synchrotron spectra all terminate in a weak but sharp peak above the main valence band edge truncated by a cut-off whose shape is determined by a convolution of instrumental broadening with the Fermi–Dirac distribution function. This cut-off defines the zero of the binding energy scale. Similar but less well resolved structure is found in the $AlK\alpha$ spectra. The observation of this structure confirms that occupation of conduction band states seen in $AlK\alpha$ spectra [7,8] to give a metallic material persists up to the near surface region probed by the low energy photoemission experiments. The conduction band structure excited at $hv = 56$ eV is shown in greater detail in Fig. 3, which also includes comparison with data taken after annealing to only 210 °C. The intensity of the conduction band photoemission increases and at the same time the valence band edge moves to higher binding energy by about 0.1 eV following the higher temperature 220 °C and 230 °C anneals. These observations are consistent with an upward shift of the Fermi level within the conduction band due to increased band occupancy. Assuming a parabolic conduction band shape and a value of $0.8\,m_0$ [6] for the conduction band electron effective mass (where m_0 is the electron rest mass) it may be inferred that the carrier concentration n increases from $1.6 \times 10^{21}\,cm^{-3}$ to $2.0 \times 10^{21}\,cm^{-3}$ as a result of the higher temperature anneals [25].

Pb 5d core level spectra for a sample with $n = 2.0 \times 10^{21}\,cm^{-3}$ are shown in Fig. 4. It may be seen that the spectrum excited at $hv = 1486.6$ eV consists of a doublet of doublets with a separation of 1.2 eV in both $5d_{5/2}$ and $5d_{3/2}$ components. There is an additional low binding
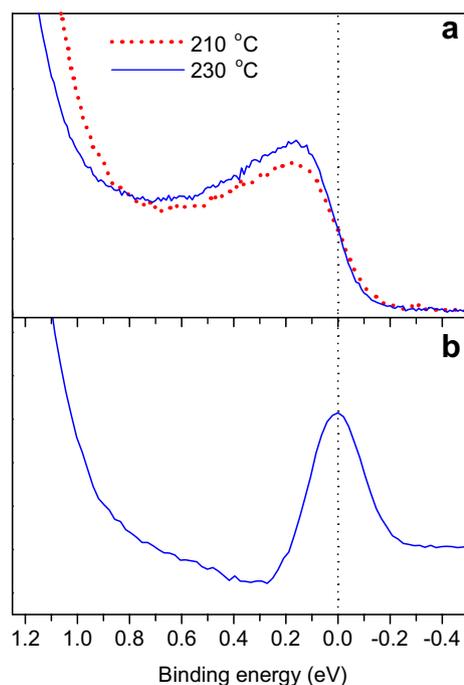

Fig. 2. Valence and shallow core Pb 5d photoemission spectra of β-PbO_2 excited at the photon energies indicated. The films have been annealed to 230 °C.

Fig. 3. (a) Structure close to the Fermi energy of excited at $hv = 56$ eV for β-PbO_2 following annealing at 210 °C and 230 °C. (b) Smoothed first derivative of the photoemission spectrum of sample annealed at 230 °C.
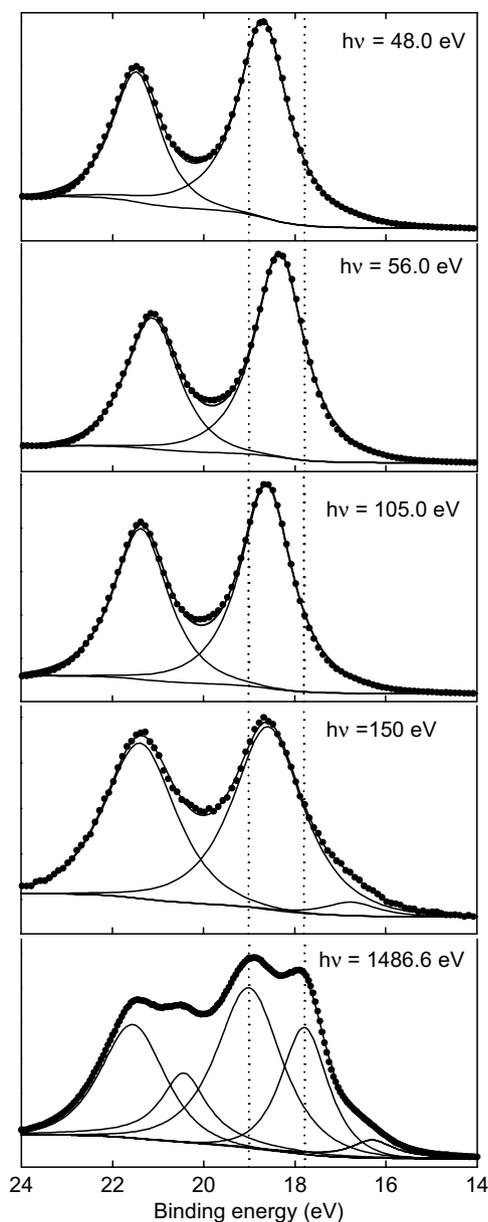
Fig. 4. Expansion of shallow core Pb 5d structure in photoemission spectra of β-PbO$_2$ excited the photon energies indicated. The data have been fitted to a series of Voigt functions.

energy shoulder associated with O 2s states. The Pb 5d core level structure is very similar to the Pb 4f core level structure reported previously [7,8]. The low binding energy Pb 5d$_{5/2}$ component is narrower than the higher binding energy component: full width at half maximum height (FWHM) values are 1.11 eV and 1.65 eV, respectively. The high binding energy component is also more dominantly Lorentzian, with contributions to the pseudo-Voigt function used to fit the spectra of 56% and 78% for low and high binding energy components, respectively. These differences may be understood in terms of lifetime broadening of the unscreened final state, or in the alternative language of the plasmon model lifetime broadening associated with the

conduction electron relaxation time. The spectra excited with lower energy synchrotron radiation differ dramatically from the Al Kα spectrum. Over the complete range of photon energies investigated the Pb 5d profile may be fitted adequately with a simple pair of spin-orbit doublets, with the addition of a single further component associated with O 2s states in the upper part of the photon energy range. The components of the doublet are found at a binding energy between that of screened and unscreened components seen in XPS, but much closer to the unscreened peak over most of the photon energy range investigated. These observations suggest that coherent metallic screening is suppressed in the near surface region probed by low energy photoemission spectroscopy, so that the spectra are dominated by unscreened final state structure. There is however a pronounced shift to low binding energy over a range of photon energies centred around 56 eV, as shown in Fig. 5. Energies in the range where the low binding energy shift is most pronounced probably coincide with the minimum in the universal curve for the photoelectron inelastic mean free path as a function of electron energy. To account for the dip to low binding energy it is further necessary to invoke a surface core level shift. Most simply this can be understood in terms of narrowing of the conduction band at the surface along with a shift in the barycentre of the conduction band spectral weight toward the valence band arising from the reduced Madelung potential at undercoordinated surface cation sites. These effects will produce a shift of the Fermi energy toward the valence band edge. Since core binding energies are all referenced to the Fermi energy this will lead in turn to a shift to low binding energy for the surface core level peak. Unfortunately the position of the bottom of the conduction band could not be identified in experimental spectra due to overlap with the tail of the valence band. The downward shift of 0.4 eV is much less than the width of the Pb 5d core level structure
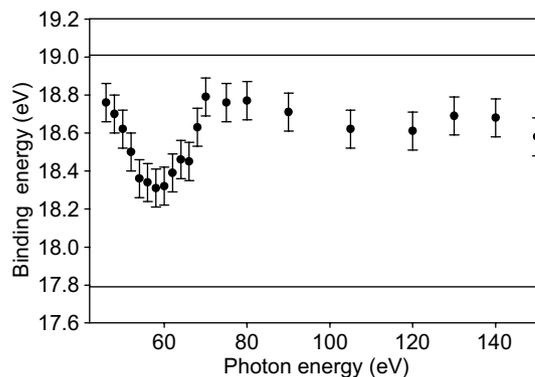

Fig. 5. Variation of binding energies for Pb 5d$_{5/2}$ structure with photon energy derived from curve fits to synchrotron excited photoemission spectra. The solid horizontal lines delineate the binding energies for screened and unscreened final state components in the Pb 5d$_{5/2}$ spectrum excited at $h\nu = 1486.6$.

(FWHM 1.3–1.8 eV depending on photon energy) and it was not possible to use curve fits to identify distinct surface and core peaks.

It is interesting to speculate as to why the alternative scenario of suppression of unscreened final state structure does not emerge. At the lowest photon energy of $hv = 40$ eV that we have used the classical escape velocity v_E of a Pb 5d photoelectron is about 1.9×10^8 cm s^{-1}. This compares with a Fermi velocity v_F for a conduction electron gas with $n = 2 \times 10^{21}$ cm^{-3} and $m^* = 0.8$ m$_0$ of only 5.6×10^7 cm s^{-1}. Thus, under our experimental conditions we are always in the limit where $v_E > v_F$ and to reach an adiabatic limit where $v_E \ll v_F$ it would be necessary to use photon energies only a couple of eV or less above the core threshold. At these photon energies the Pb 5d core lines sit on a strong inelastic background and it is not possible to characterise the core lineshape with confidence.

In summary we have studied photoemission spectra of metallic β-PbO$_2$ with excitation over a photon energy range between 40 eV and 150 eV. A sharp conduction band feature is observed in all spectra, confirming that conduction band occupancy persists up to the near surface region. In contrast to spectra excited with Al Kα radiation, the Pb 5d core line excited with VUV synchrotron radiation consists of a simple spin-orbit doublet with no evidence of structure due to metallic final state screening over the complete photon energy range between 40 eV and 150 eV. In addition there is evidence of a surface core shift for photon energies centred around the minimum in the universal curve for electron inelastic mean free paths. The current work adds to the recent finding from hard XPS that coherent screening is suppressed close to surfaces [16–19] but further theoretical work is needed to explain the physics of this effect.

References

[1] R.D. Shannon, R.X. Fischer, Phys. Rev. B 73 (2006) 235111.
[2] Semiconductors: Physics of Non-Tetrahedrally Bonded Binary Compounds IIO. Madelung (Ed.), Landolt-Börnstein, New Series, Group III, vol. 17, Pt. f, Springer Verlag, Berlin, 1984.
[3] W. Mindt, J. Electrochem. Soc. 116 (1969) 1076.
[4] P.T. Moseley, J.L. Hutchison, M.A.M. Bourke, J. Electrochem. Soc. 129 (1982) 876.
[5] M. Heinemann, H.I. Terpstra, C. Haas, R.A. de Groot, Phys. Rev. B 52 (1995) 11740.
[6] J.P. Pohl, G.L. Schlectriemen, J. Appl. Electrochem. 14 (1984) 521.
[7] D.J. Payne, R.G. Egdell, W. Hao, J.S. Foord, A. Walsh, G.W. Watson, Chem. Phys. Lett. 411 (2005) 181.
[8] D.J. Payne et al., J. Mat. Chem. 17 (2007) 267.
[9] A. Kotani, Y. Toyazawa, J. Phys. Soc. Jpn. 37 (1974) 912.
[10] R.G. Egdell, J. Rebane, T.J. Walker, D.S.L. Law, Phys. Rev. B 59 (1999) 1792.
[11] R.G. Egdell, T.J. Walker, G. Beamson, J. Elec. Spec. Rel. Phen. 128 (2003) 59.
[12] V. Christou, M. Etchells, O. Renault, P.J. Dobson, O.V. Salata, G. Beamson, R.G. Egdell, J. Appl. Phys. 88 (2000) 5180.
[13] P.A. Glans et al., Phys. Rev. B 71 (2005) 235109.
[14] Y. Gassenbauer, R. Schafranek, A. Klein, Phys. Rev. B 73 (2006) 245312.
[15] J.N. Chazalviel, M. Campagna, G.K. Wertheim, H.R. Shanks, Phys. Rev. B 16 (1977) 697.
[16] G. Pannacione et al., Phys. Rev. Lett. 97 (2006) 116401.
[17] K. Horiba et al., J. Electron Spectrosc. Relat. Phenom. 144–147 (2005) 557.
[18] H. Tanaka et al., Phys. Rev. B 73 (2006) 094403.
[19] M. Taguchi et al., Phys. Rev. Lett. 95 (2005) 177002.
[20] J.E. Inglesfield, J. Phys. C 16 (1983) 403.
[21] L. Hedin, J. Michelis, J. Inglesfield, Phys. Rev. B 58 (1998) 15565.
[22] A.B. Velichenko, R. Amadelli, A. Benedetti, D.V. Girendko, S.V. Kovalyov, F.I. Danilov, J. Electrochem. Soc. 149 (2002) C445.
[23] S. Abaci, K. Pekmez, T. Hőkelek, A. Yildiz, J. Power Sources 88 (2000) 232.
[24] A. Howard, D.N.S. Clark, C.E.J. Mitchell, R.G. Egdell, V.R. Dhanak, Surf. Sci. 518 (2002) 210.
[25] See Ref. [7] for the procedure used to estimate carrier concentrations.